ICES Journal of Marine Science, 60: 1381–1391. 2003
doi:10.1016/S1054–3139(03)00142-5

Modelling the effect of swimbladder compression on the acoustic backscattering from herring at normal or near-normal dorsal incidences

Natalia Gorska and Egil Ona

Gorska, N., and Ona, E. 2003. Modelling the effect of swimbladder compression on the acoustic backscattering from herring at normal or near-normal dorsal incidences – ICES Journal of Marine Science, 60: 1381–1391.

Inaccuracy in herring target strength can be an important source of bias in the acoustic assessment of several important herring stocks. New acoustic data on herring target strength (Ona *et al.*, 2001, submitted for publication; Ona, 2003) confirm previous suggestions and evidence on a possible reduction of the size of the herring swimbladder as a result of its compression with increasing water depth. Theoretical work for a better understanding of the acoustic scattering from herring over its entire depth distribution may therefore be essential for improving abundance estimation. This study supplements the analysis, conducted by Gorska and Ona (2003) for herring averaged-backscattering cross-section. The modal-based, deformed-cylinder model (MB-DCM) solutions, presented in that paper, are used. The sensitivity of the herring backscattering cross-section in case of normal or near-normal dorsal incidences is studied with respect to frequency, contraction factors of the swimbladder dimensions and some fish morphological parameters. The study is important for a better understanding of not only the backscattering by individual fish for the dorsal incidence, but also the depth- and frequency-dependencies of the mean-backscattering cross-section. The theoretical results have been applied in the interpretation of the actual measured target-strength data on adult herring.

Keywords: depth-dependent target strength, herring, modelling, normal or near-normal dorsal incidences, swimbladder compression.

Received 26 August 2002; accepted 10 July 2003.

N. Gorska; Institute of Oceanology of Polish Academy of Sciences, ul. Powstancow Warszawy 55, PL-81-712 Sopot, Poland. E. Ona: Institute of Marine Research, PO Box 1870, Nordnes, N-5817 Bergen, Norway; tel: +47 55 23 85 00; fax: +47 55 23 85 84; e-mail: egil.ona@imr.no. Correspondence to N. Gorska; tel: +48 58 551 72 81; fax: +48 58 551 21 30; e-mail: gorska@iopan.gda.pl.

List of symbols

$a_{sb}(x, z)$ and $l_{sb}(z)$	-cross-section radius and major-axis length of swimbladder prolate spheroid;
$a_0^{sb}(z)$	-semi-minor-axis length of swimbladder prolate spheroid;
$a_b(x)$ and l_b	-cross-section radius and major-axis length of fish-body prolate spheroid;
x	-co-ordinate, along-major axis of prolate spheroid;
z	-depth;
$h_{sb} = c_{sb}/c$	-swimbladder sound-speed contrast;
$g_{sb} = \rho_{sb}/\rho$	-swimbladder-density contrast;
ρ_{sb} and c_{sb}	-gas density and sound speed of swimbladder, respectively;
ρ and c	-density and sound speed of surrounding seawater;
$h_b = c_b/c$	-body sound-speed contrast;
$g_b = \rho_b/\rho$	-body-density contrast;
ρ_b and c_b	-density and sound speed of fish body, respectively;
$k = 2\pi f/c$	-wave number in surrounding seawater;
f	-echo-sounder frequency;

1054–3139/03/121381+11 $30.00

α and β	-contraction factors of swimbladder semi-minor and major axes length, respectively;
$\eta = \alpha + \beta$	-contraction factor of swimbladder dorsal cross-section area;
$f_{sb}(z) = \lvert f_{sb}(z) \rvert \ \exp(i\Phi_{sb}(z))$	-backscattering length of swimbladder;
$f_b(z) = \lvert f_b \rvert \ \exp(i\Phi_b)$	-backscattering length of fish body;
f_{tot}	-backscattering length of whole fish;
$\sigma_{bsc}(z)$	-backscattering cross-section of whole fish;
TS(z)	-target strength of whole fish;
δ	-spatial displacement between centres of cross-sections of swimbladder and fish-body prolate spheroids;
$\sigma_{int}(z)$	-term, responsible for interference between echoes from body and swimbladder.

Introduction

The abundance of the Norwegian spring-spawning herring stock has been carefully monitored by acoustic surveys since its reappearance after collapsing in the late 1960s (Dragesund *et al.*, 1980; Røttingen *et al.*, 1994; Johannessen *et al.*, 1995). The assessment of the stock is based on the results from acoustic surveys of the spawning area, the wintering area and the feeding grounds, which significantly differ in fish behaviour, density and depth distribution. Discrepancies in the acoustic estimates of biomass, presumed to be similar, were observed for these areas. Several sources of bias have been considered to explain the survey results (Røttingen *et al.*, 1994), among which vessel avoidance and inaccuracy in target strength are considered to be the most important.

New data on herring target strength (Ona *et al.*, 2001, submitted for publication; Ona, 2003) confirm earlier speculations (Blaxter and Batty, 1984; Ona, 1990; Huse and Ona, 1996) on herring target strength being depth- or pressure-dependent. The correction of herring abundance estimates by applying the new, pressure-dependent target strength (Vabø, 1999; Ona *et al.*, submitted for publication) may significantly decrease the discrepancies observed in the acoustic-abundance estimates. It also encourages a deeper theoretical and experimental study of the acoustic scattering by herring with a depth-compressed swimbladder.

This was the main motivation for our earlier paper (Gorska and Ona, 2003), in which the depth-dependent, averaged-backscattering cross-section of herring was studied. The main parameters controlling the backscattering were discussed. The modelling results were compared with the *measured* averaged-backscattering cross-section data. The importance of the swimbladder compression in the explanation of the measured, depth-dependent herring target strength was demonstrated. The present paper supplements the previous study. Here the depth-dependent, backscattering cross-section of individual herring at normal or near-normal dorsal incidences is considered in detail. The terms "dorsal-aspect backscattering cross-section" and "dorsal incidence" will be used in case of normal or near-normal dorsal incidences, for which the backscattering cross-section reaches a maximum. The analysis of the dorsal-incidence case for individual fish improves the understanding of the main parametric dependencies obtained in the echo-average case (Gorska and Ona, 2003). Moreover, the previous study of mean-backscattering cross-section demonstrated, in its comparison to the data, how the individual swimbladder dimensions may vary with depth. The data for dorsal incidence were also subtracted (Ona *et al.*, submitted for publication). They may be useful in elucidating the character of the depth-contracted, swimbladder deformation.

In this paper the sensitivity of the depth-dependence of the dorsal-aspect, backscattering cross-section to the acoustical (frequency) and body parameters (fish morphology and the contraction factors of the swimbladder's dimensions) is studied. Definitions of the symbols used in the equations are given above. The same approach as that of Gorska and Ona (2003) is used. The backscattering cross-sections of the whole fish, the fish body and the swimbladder are considered, together with a term describing the interference between echoes from the swimbladder and the body. The numerical results are compared with the measured dorsal-aspect, backscattering cross-section data.

Materials and methods

Using the modal-based, deformed-cylinder model (MB-DCM) (Stanton, 1989), analytical solutions for the backscattering lengths of swimbladder $f_0^{sb}(z)$ and fish body f_0^b were obtained in Gorska and Ona (2003). The swimbladder and fish body were modelled as gas- and liquid-filled prolate spheroids, respectively (Figure 1a). The present study is based on the solution for the backscattering length of the swimbladder (Equation (7)) together with the modal coefficients (Equation (9)) and the expression for the backscattering length of the fish body (Equation (8)) with the modal coefficients (Equation (10)) from Gorska and Ona (2003). The only symbol differences between that study and this one are that we describe the swimbladder and body backscattering lengths as f_{sb} and f_b, respectively, instead of using $f_0^{sb}(z)$ and f_0^b.

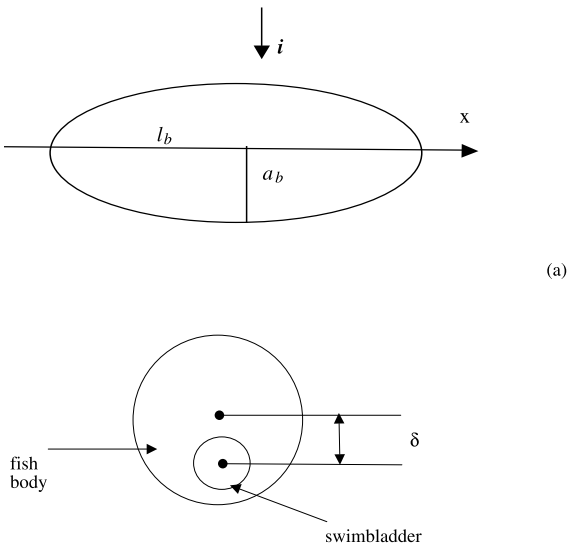

Figure 1. (a) Prolate-spheroid geometry of fish body. (b) Fish transversal cross-section.

In Gorska and Ona (2003) the interference between echoes from the swimbladder and the fish body was neglected and the averaged whole-fish, backscattering cross-section was computed as the sum of the swimbladder and body backscattering cross-sections. However, the echo interference is important in the case of backscattering by an individual fish. We consider the whole-fish backscattering length, f_{tot}, as the sum of the backscattering lengths from the fish body, f_b, and the swimbladder, f_{sb}. It is expressed as:

$$f_{tot}(z) = f_{sb}(z)\exp(i2k\delta/h_b) + f_b \quad (1)$$

where δ describes the spatial displacement between the centres of the cross-sections of the swimbladder and the fish-body prolate spheroids (Figure 1b).

Stanton's (1989) MB-BCM solution, used for f_b and f_{sb}, has been developed assuming that the axis coincides with the lengthwise axis of the scatterer. Noting, however, that the z-axis of a cylindrical co-ordinate system coincides with the lengthwise axis of the fish body and does not coincide with the longitudinal axis of the swimbladder, we have introduced the additional phase-shift $2k\delta/h_b$ in the backscattering length of the swimbladder in Equation (1).

It is important to remember that the tilt of the swimbladder axis relative to the snout–tail axis of the fish is ignored in the coefficients of MB-DCM modal sum for the swimbladder (Equation (9) in Gorska and Ona, 2003). The microtome longitudinal section presented in Figure 2 confirms this assumption.

The differential-backscattering cross-section of whole fish can be presented as:

$$\begin{aligned}\sigma_{bsc}(z) &= |f_{sb}(z)\exp(i2k\delta) + f_b|^2 \\ &= \sigma_{sb}(z) + \sigma_b + \sigma_{int}(z)\end{aligned} \quad (2)$$

where the functions $\sigma_{sb}(z) = |f_{sb}(z)|^2$ and $\sigma_b = |f_b|^2$ denote the differential-backscattering cross-sections of the swimbladder and the body, respectively. The term responsible for the echo interference is expressed as $\sigma_{int}(z) = 2|f_{sb}(z)||f_b|\cos(2k\delta/h_b + \Phi_{sb}(z) - \Phi_b)$, where $\Phi_{sb}(z)$ and Φ_b describe the phases of the swimbladder and fish-body backscattering lengths, respectively. Two last terms in Equation (2) describe the fish-body contribution to the whole-fish backscattering.

Target strength is related to the backscattering cross-section by the relationship:

$$TS(z) = 10\log\sigma_{bsc}(z) \quad (3)$$

As was discussed in Gorska and Ona (2003), the volume of the herring swimbladder is compressed with depth, according to Boyle's law (Ona, 1990), but the exact nature of this change in swimbladder dimensions with depth is not yet clear. Therefore, following that paper we used Equations (13) and (14) to describe depth-dependencies of the dimensions as:

$$a_0^{sb}(z) = a_{sb}(0)(1 + z/10)^{-\alpha} \quad (4)$$

$$l_{sb}(z) = l_{sb}(0)(1 + z/10)^{-\beta} \quad (5)$$

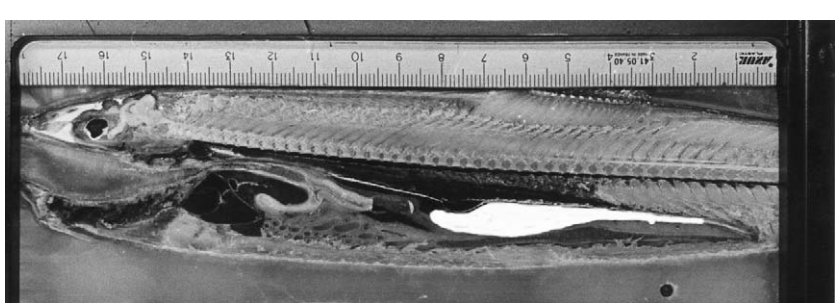

Figure 2. Microtome longitudinal section of a 32 cm herring. The air-filled main chamber of the swimbladder is shown in white.

Results and discussion

The backscattering cross-section of individual fish at dorsal incidence was only analysed briefly in our previous paper (Gorska and Ona, 2003). Moreover, the comparison between the dorsal incidence and the averaged characteristics was made at 38 kHz only (Figures 1b and 3a, Gorska and Ona, 2003). However, the dorsal-incidence study is important for a better understanding of the backscattering by individual fish and the explanation of the echo-average results. Therefore, in this section we analyse numerically the parameters controlling backscattering by individual fish at dorsal incidence.

Depth-dependence: echo-sounder frequency

Figure 3 illustrates the depth-dependence of $4\pi\sigma_{sb}$ (Figure 3a) and $4\pi\sigma_{bsc}$ (Figure 3c), including the depth-dependence of the term $4\pi\sigma_{int}$ describing the interference between the waves scattered by the fish body and the swimbladder (Figure 3b). Calculations were made at the frequencies 18, 38, 120 and 200 kHz. Computations were performed for a herring with total length 32 cm, where the ratio of the swimbladder length to the total length is set to 0.26 (see Figure 2) and the dorsal width of swimbladder and fish body to 10 and 20 mm, respectively. The density and sound-speed contrasts used are (1.04, 1.04) and (0.00129, 0.23) for the fish body and the fish swimbladder, respectively. Contraction factors α and β (Equations (4) and (5)) equalled 1/3. The spatial displacement δ, assumed to be constant along the fish's longitudinal axis, was 10 mm.

Figure 3a demonstrates that herring swimbladder-backscattering cross-section decreases rapidly with depth, by about one order of magnitude, over the entire frequency range investigated. To explain the influence of frequency on the backscattering by swimbladder, the dependence of the backscattering length, normalized by swimbladder length, on ka_0^{sb} has been analysed. The computations were based on Equations (7), (9) and (11) in Gorska and Ona (2003), in which the depth-swimbladder contraction is neglected and $a_{sb}(x, z)$ is the function of x only. Further, the range of variability in ka_0^{sb}, as caused by swimbladder compression, has been calculated at different frequencies (Figure 5). To obtain this, the depth-dependence of the swimbladder's semi-minor-axis length, a_0^{sb} (Equation (4)), with contraction factor $\alpha = 1/3$, was used. According to Figure 5, ka_0^{sb} varies from 0.377 ($z = 0$ m) to 0.120 ($z = 300$ m) at 18 kHz. As shown in Figure 4 this change causes variability in the normalized backscattering length modulus from 0.425 to 0.332. The respective ranges for the other three frequencies are also shown. The right and left bounds of each range refer to the depth $z = 0$ m and $z = 300$ m, respectively. Figure 4 demonstrates that

(i) the range corresponding to 18 kHz occupies the lower part of the curve;
(ii) the curve level for the right bound of the range at 200 kHz is lower than that for the right bound at 120 kHz, while the relative positions for the left bounds are opposite.

These features explain the facts that (Figure 3a):

(i) the smallest backscattering cross-section is observed at 18 kHz over the entire depth range and
(ii) the largest σ_{sb} is found at 120 kHz at depths less than 60 m and at 200 kHz at greater depths.

Figure 3b represents the depth-dependence of the term describing the interference between echoes from the fish swimbladder and body. This term is proportional to the swimbladder-backscattering length modulus $|f_{sb}(z)|$. However, the comparison with Figure 3a, where the $|f_{sb}(z)|^2$ depth-variation is presented, indicates that the $\sigma_{int}(z)$ depth-dependence does not repeat the depth-dependence of $|f_{sb}(z)|$. This discrepancy is explained by the effect of the depth-dependent phase $\Phi_{sb}(z)$ of the echo from swimbladder. The phase depends on the geometric shape of the insonified swimbladder surface, which varies with depth during the contraction. Analysing Figure 3b, we may also conclude that the depth-dependence of σ_{int} is sensitive to frequency. The frequency sensitivity of the phase $(2k\delta/h_b + \Phi_{sb}(z) - \Phi_b)$ is important for understanding this.

Comparing the curves in Figure 3c with the respective curves for the swimbladder in Figure 3a, a significant difference can be seen. This is explained by the fact that the depth-dependence of the whole-fish backscattering cross-section is defined not only by the depth-variability of swimbladder-backscattering cross-section alone, but also by the variable interference term σ_{int}. In other words, the variability of both the modulus $|f_{sb}(z)|$ and the phase $\Phi_{sb}(z)$ of swimbladder-backscattering length is important. The influence of the echo-sounder frequency on the depth-dependence of the whole-fish backscattering is also demonstrated.

This analysis is important for understanding the depth- and frequency-dependencies of the averaged-backscattering cross-section, studied in Gorska and Ona (2003). The discrepancies with the dorsal-incidence case are explained by the effect of the depth and frequency variability of the swimbladder-directivity pattern. To understand the difference in the depth-dependencies, it should be noted that the swimbladder-directivity pattern width can increase with depth due to swimbladder-length contraction. This leads to an increase in the convolution of fish directivity pattern and the fish orientation distribution with depth at the selected range of acoustical and fish parameters. Therefore, the swimbladder mean-backscattering cross-section decreases more slowly with depth than the dorsal-aspect backscattering cross-section.

Depth-dependence: contraction factors α and β

It was shown in Gorska and Ona (2003) that the sensitivity analysis, with respect to the contraction factors α and β,

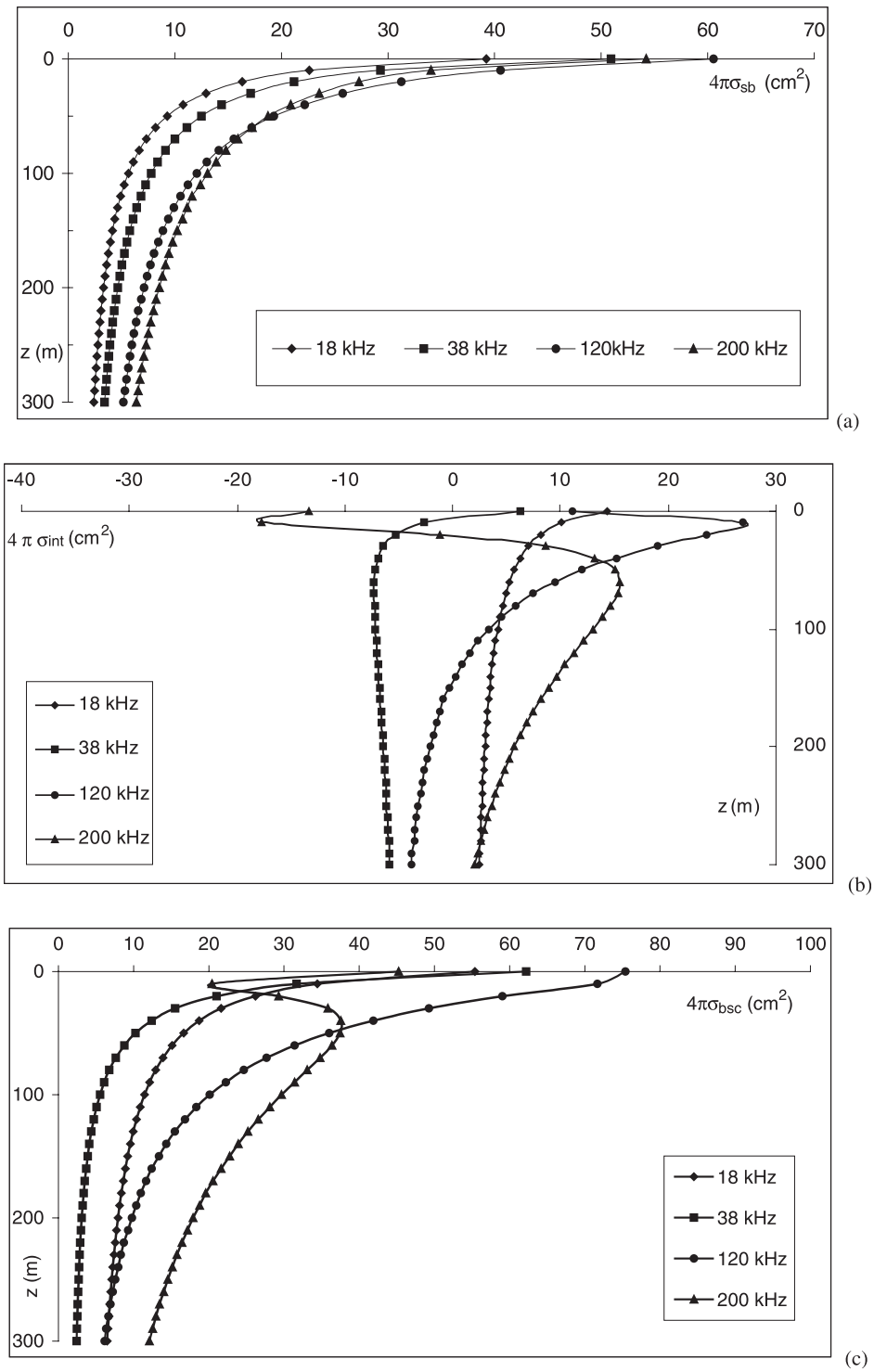

Figure 3. Depth-dependence of (a) the swimbladder-backscattering cross-section, (b) the term responsible for the interference of the echoes from the swimbladder and the fish body, and (c) the whole-fish backscattering cross-section. Computations are made for 18, 38, 120, and 200 kHz. The calculation parameters are: total-fish length $l_b = 32$ cm; the ratio of the swimbladder length to the total length $l_{sb}/l_b = 0.26$; dorsal width of swimbladder and fish body – $2a_0^{sb}(z = 0) = 10$ mm and $2a_b = 20$ mm, respectively; density and sound-speed contrasts are (1.04, 1.04) and (0.00129, 0.23) for the fish body and the fish swimbladder, respectively. Semi-minor and major axes lengths decrease with depth with equal contraction factors $\alpha = \beta = 1/3$. The spatial displacement, δ, equals 10 mm. The values of 4π times the differential cross-section (cm^2) are indicated on the horizontal axis.

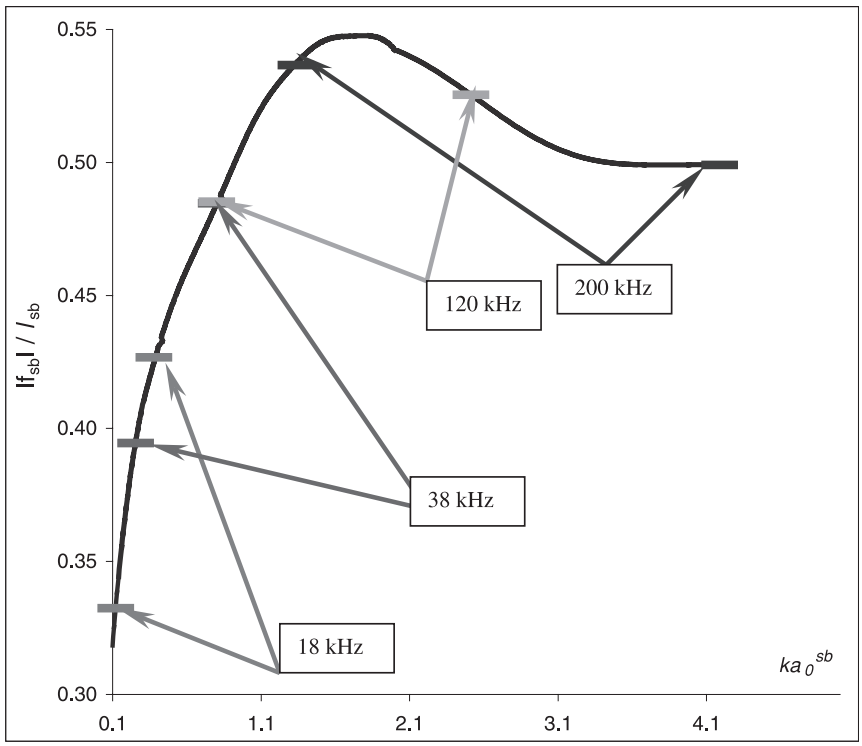

Figure 4. Dependence of the backscattering length modulus, normalized by swimbladder length, on parameter $ka_0{}^{sb}$ for the fish swimbladder. Density and sound-speed contrasts for the swimbladder are 0.00129 and 0.23, respectively.

is helpful in data interpretation and the understanding of how herring-swimbladder dimensions are compressed with depth. The data for the dorsal incidence were also extracted from individual tracks (Ona *et al.*, submitted for publication). For their explanation, the sensitivity analysis seems to be reasonable.

The results of the numerical study for herring swimbladder at 38 kHz are presented in Figure 6a. These computations were made for the same three selected cases, viz. (i) $\alpha = 1/3$, $\beta = 1/3$, (ii) $\alpha = 2/5$, $\beta = 1/5$ and (iii) $\alpha = 1/2$, $\beta = 0$, as the ones for the averages. Other computed parameters are the same as those given in Figure 3. It is important to remember that in case (i), all three swimbladder dimensions have similar contraction factors and the proportions between the relative dimensions have been maintained during the contraction. The length reduction is smaller or the length is a constant value in cases (ii) and (iii), respectively.

Remembering that the contraction factor for the swimbladder dorsal cross-section area, η, is largest ($\eta = 2/3$) and smallest ($\eta = 1/2$) for the cases (i) and (iii), respectively, we can conclude that as in the case of the averages, the depth-dependence of the swimbladder-backscattering cross-section is controlled by this parameter. As expected, depth-dependence is steeper for larger contraction factors of the dorsal geometric cross-section.

The comparison with the averaged-backscattering cross-section (not presented here) demonstrated that:

(a) the depth-dependence is steeper for the dorsal incidence in cases (i) and (ii) and
(b) the dependencies are the same in case (iii), in which swimbladder length does not vary with depth, at all selected frequencies. This is explained by the depth-variability of swimbladder-directivity pattern discussed above.

Depth-dependence: spatial displacement between swimbladder and fish body

As was noted above the interference between the echoes from fish swimbladder and body can influence backscattering from whole fish and, since the echo interference is sensitive to fish morphology, it is therefore reasonable to study sensitivity of total backscattering cross section to the morphological parameters. The influence of the spatial displacement between swimbladder and fish body, δ, was analysed. The calculations were made at the selected frequencies for δ with values of 8, 10, 12 and 14 mm. The results for 38 kHz are presented in Figure 6b. The whole-fish backscattering cross-section is sensitive to δ, which defines the rate of σ_{bsc} depth-variation and σ_{bsc}-level. A similar conclusion can be made for the other frequencies. The calculations also demonstrate the

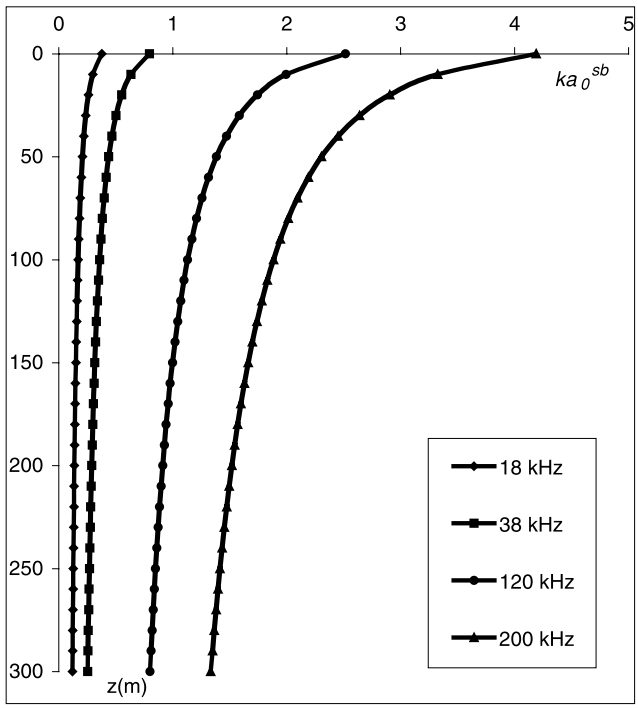

Figure 5. Dependence of ka_0^{sb} parameter on the depth, z, for four frequencies. The semi-minor-axis length varies with depth according to Equation (4) with contraction factor $\alpha = 1/3$. The swimbladder dorsal width is 10 mm.

sensitivity of the frequency-dependence of the whole-fish backscattering cross-section to the distance δ, but this is not presented here.

The body contribution to whole-fish backscattering

In Equation (2), the term $\sigma_b + \sigma_{int}(z)$ describes the fish-body influence on backscattering from the whole fish. To evaluate the importance of this factor we calculated two ratios, $\sigma_b/\sigma_{sb}(z)$ and $\sigma_{int}(z)/\sigma_{sb}(z)$, thereby enabling a comparison of the fish body and the swimbladder contributions to the whole-fish backscattering. The results of this study are summarized in Figure 7a and b, in which the depth-dependencies of the ratios at various frequencies are presented. The simulation parameters were the same as used in Figure 3.

With regard to the averages (Gorska and Ona, 2003), the analysis shows that the $\sigma_b/\sigma_{sb}(z)$ increases with depth (Figure 7a), because of the gradually decreased scattering from the swimbladder with depth, and depends on frequency. The ratio $\sigma_{int}(z)/\sigma_{sb}(z)$ also varies with depth and frequency (Figure 7b). The calculations demonstrate that both terms, σ_b and $\sigma_{int}(z)$, can be comparable to $\sigma_{sb}(z)$ at greater depths. Therefore, the fish-body contribution to the backscattering by the whole fish varies with depth and frequencies and can be important for greater depths.

Comparison with measurements and discussion

In this section, the theoretical results obtained are compared to *in situ* target-strength data. These data were collected in November 1997 from Vestfjord and Ofotfjord, within the wintering area of the Norwegian spring-spawning herring (Ona *et al.*, submitted for publication). Target-strength measurements were conducted using a 38 kHz, pressure-stabilized, submersible, downward-facing, split-beam transducer, lowered into or close to the herring layers. Measurements were made over a depth range of 40–300 m, covering most of the vertical-distribution range for herring, where an extremely narrow fish-length distribution was observed. The mean length and the ratio of the standard deviation to the mean length were 32 cm and 0.04, respectively. Target-strength depth-dependence was studied in detail on the basis of the processed data.

The single-fish traces can be observed as a connected series of single-target detections. Making the assumption that the maximum target strength of a fish is reached when it is nearly horizontal, these values were extracted from the selected tracks. Only the tracks with a definite change from a slight positive to slight negative tilt (or the opposite), during passage through the acoustic beam, were selected for the analysis. The mean value of 200 maximum target-strength values was recorded for each 10-m depth interval.

Two theoretical solutions have been compared to the collected data. Firstly we made a comparison of the solution (Equation (2)), in which the interference between echoes from the swimbladder and the body is included. It has been demonstrated that the calculated depth-dependent target strengths are lower than the observed ones. For this

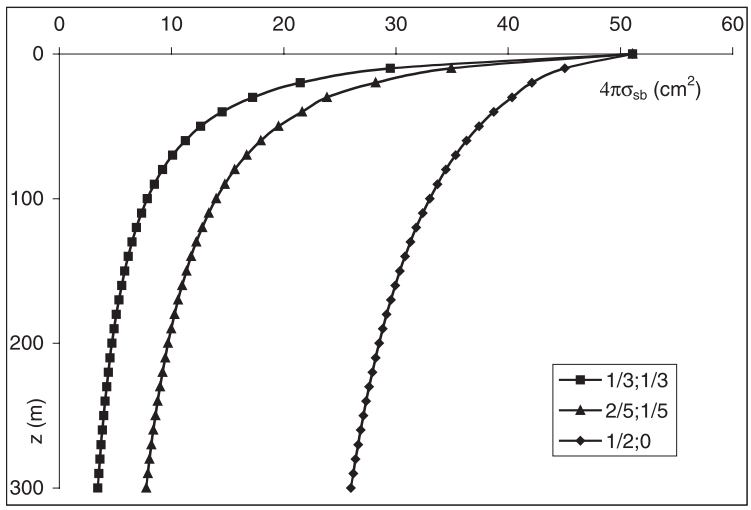

(a)

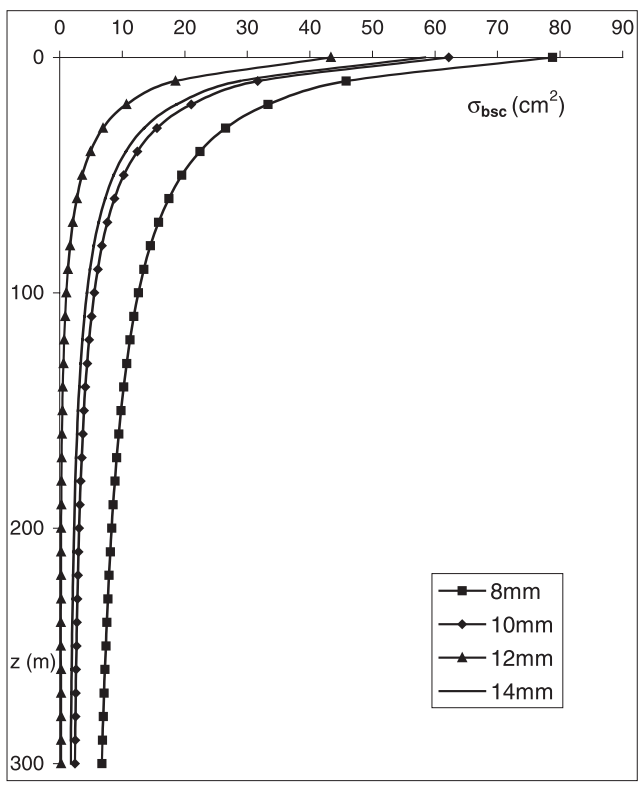

(b)

Figure 6. Sensitivity of the depth-dependence of the swimbladder-backscattering cross-section to the contraction factors of individual dimensions of the swimbladder (a) (the values of α and β are presented in the legend) and to the displacement δ (b). The calculations are made at the frequency of 38 kHz. Other computation parameters are the same as those given in Figure 3.

reason we also compared the measured data to the backscattering cross-section which we calculated as the incoherent sum of swimbladder and body backscattering cross-sections neglecting the echo interference: $\sigma_{bsc}(z) = \sigma_{sb}(z) + \sigma_b$. The comparison is shown in Figure 8. Here, the maximum target-strength data (black points) have been fitted by non-linear regression to a swimbladder-compression model. The regression curve is presented in Figure 8

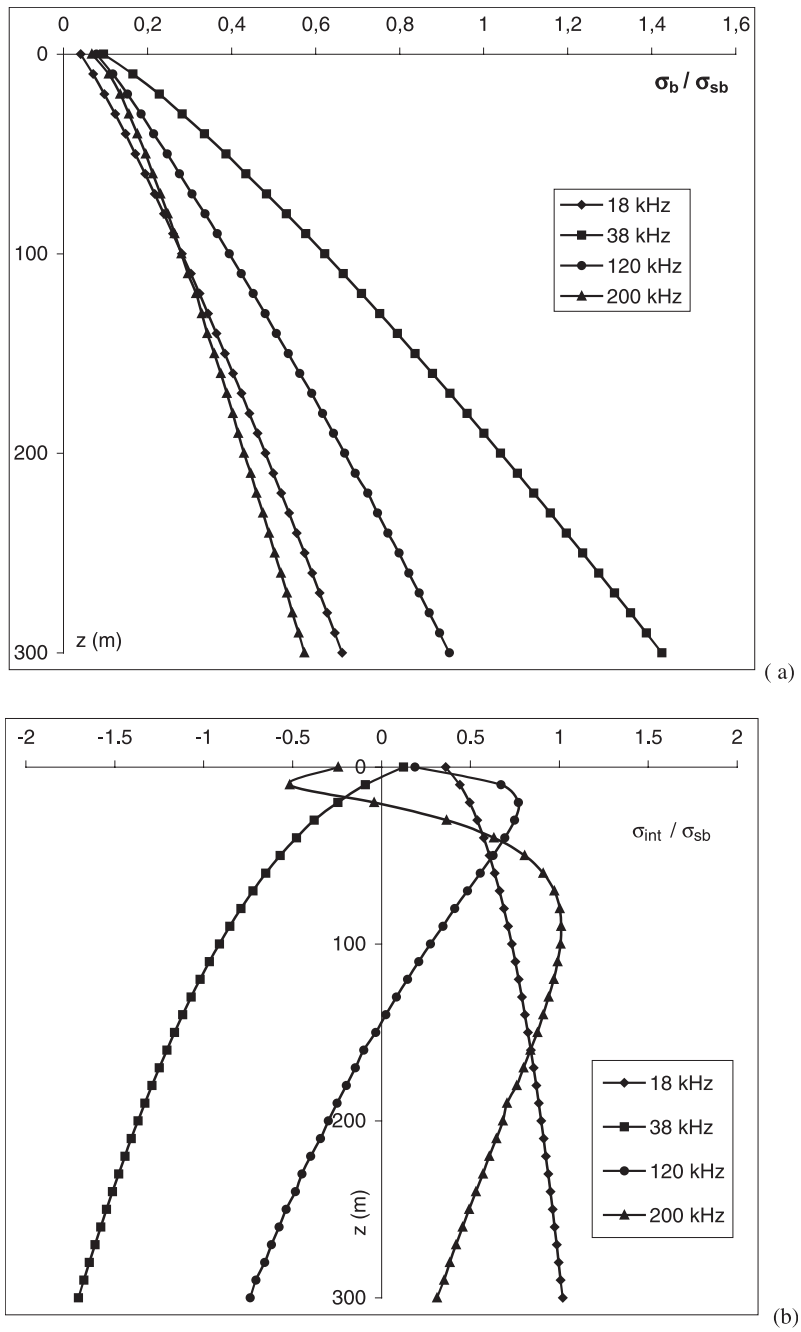

Figure 7. The depth-dependent contribution of the fish body at various frequencies: (a) the depth-dependence of the ratio $\sigma_b/\sigma_{sb}(z)$ and (b) the ratio $\sigma_{int}(z)/\sigma_{sb}(z)$ at 18 kHz (squares on curve), 38 kHz (diamonds), 120 kHz (triangles) and 200 kHz (circles). The simulation parameters are the same as those given in Figure 3.

by the non-marked curve. The model is given by equations (6) and (7) in Ona *et al.* (2003). It can be presented as:

$$\sigma_{bsc}(z) = \sigma_0(1 + z/10)^{\gamma} \quad (6)$$

and

$$TS(z) = TS_0 + 10\gamma \log(1 + z/10) \quad (7)$$

where $\sigma_0 = 52.7\ cm^2$, $TS_0 = -33.8$ dB and $\gamma = -0.20$.

Two other curves correspond to the MB-DCM computations for the whole fish with the selected contraction factors of swimbladder semi-minor and major axes: $\alpha = 1/3$, $\beta = 1/3$ (diamonds) and $\alpha = 1/2$, $\beta = 0$ (triangles).

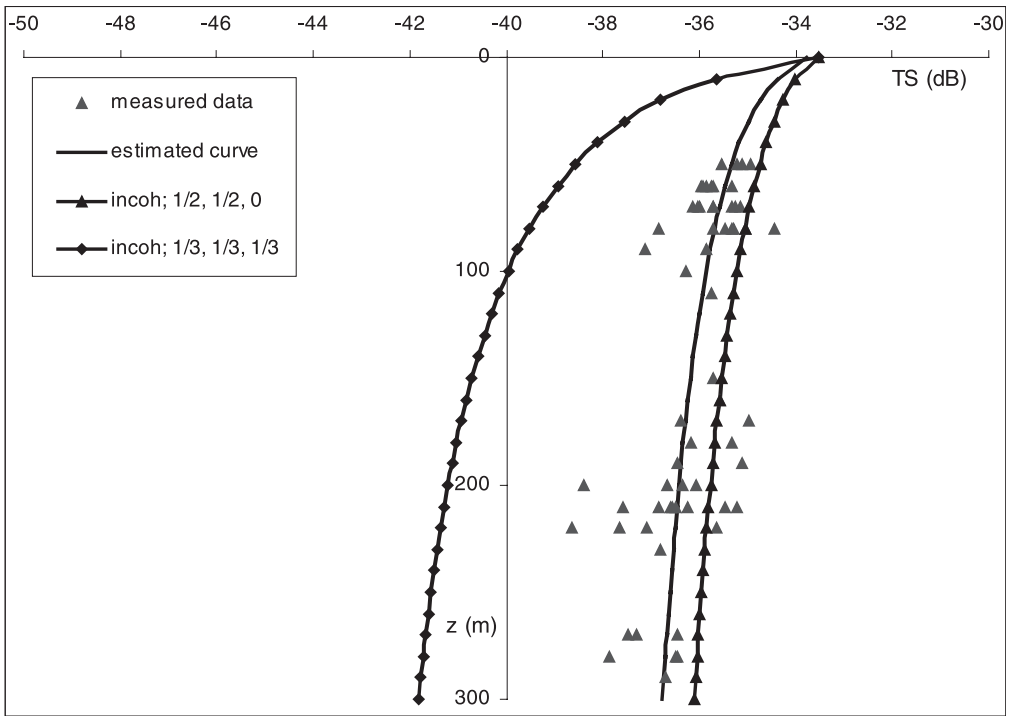

Figure 8. A comparison with experimental data at 38 kHz. The measured data (black points) and the fitted compression model (non-marked curve) (Ona *et al.*, submitted for publication) are presented. Other curves refer to the MB-DCM computations made for the whole fish for different contraction factors of the semi-minor and major axes as indicated in the legend. The other simulation parameters are the same as those given in Figure 3. The echo interference between the swimbladder and the fish body is neglected in the calculations.

The other simulation parameters are the same as those given in Figure 3.

For the first curve, the swimbladder length and width are compressed at the same contraction factor. For the second curve, the swimbladder length is fixed. It can be shown that all solutions, where the swimbladder length contracts less than the width, occupy the domain between the two indicated curves: in the opposite case the curves are located outside the domain. All the measured data also occupy the area inside this domain. Summarizing, this actually suggests how the swimbladder contracts with depth: the length reduces with pressure less than the width. Such a result is in good agreement with the findings of Blaxter (1979) and Ona (1990), each of which demonstrated a smaller change in the swimbladder's horizontal dimension compared to its vertical dimension. Figure 8 also supports the idea that the observed depth-dependence of herring target strength can be explained by depth compression of herring swimbladder.

The good fit with the collected data of $\sigma_{bsc}(z)$, calculated as the incoherent sum of $\sigma_{sw}(z)$ and σ_b, and a disagreement in a case of the coherent summation (Equation (2)) mean that the interference between the echoes from the swimbladder and the body is not important in the explanation of the measured data. Two reasons can be suggested: first, the high sensitivity of the interference term to the morphology, as it was demonstrated in the previous section, and second, the way the data were collected. Each data point has been obtained as the average of the echoes from different fish. Fish differ in shape and their shapes may be imperfect. Because of echo-interference sensitivity to the morphology, the averaging smears the coherence of the "phases" and makes the backscattering incoherent.

Summary

The depth-dependence of herring target strength for dorsal incidence has been studied theoretically using the MB-DCM. The sensitivity to the frequency, individual swimbladder-dimension-contraction factor and fish morphology (the swimbladder's spatial position inside the fish body) has been analysed. The results have been used to explain the main dependencies for the averaged-backscattering cross-section (Gorska and Ona, 2003). A comparison to the measured, maximum-backscattering cross-section data has been made. Summarizing the study, the following can be concluded:

1. The depth-dependence of the herring swimbladder and the whole-fish backscattering cross-sections is significant and is sensitive to the frequency. The frequency-dependence of the backscattering cross-sections for the swimbladder and the whole-fish varies with depth. The

spatial displacement between swimbladder and fish body may influence the depth- and frequency-dependencies of the backscattering cross-section.
2. The importance of the depth- and frequency-dependent herring-directivity pattern in the interpretation of the depth- and frequency-dependencies of the averaged-backscattering cross-section has been demonstrated.
3. It has been shown that in the case of individual fish the interference of echoes from the swimbladder and the fish body can be important, influencing the depth- and frequency-dependencies of the whole-fish backscattering cross-section.
4. The comparison with the measured data has demonstrated that the swimbladder was not compressed ideally. The length of the swimbladder is probably fixed and most of the volume change must occur in the height/width dimensions of the swimbladder. This supports the conclusion of the comparison made for the averaged data in Gorska and Ona (2003).

In this paper we do not consider the complicated morphology of herring, but describe the swimbladder and the fish body as simple, geometric shapes; viz. prolate spheroids. However, the analysis, based on the model, suggests that further studies will require information on real-fish morphology and also how the compressed-swimbladder dimensions change. We consider therefore the present study as a first step towards the application of finite-element modelling, which also allows for the use of detailed data on the fish and swimbladder morphology. New and exciting fish-compression experiments are planned for the reconstruction of the herring-swimbladder shape under pressure.

Acknowledgements

The authors greatly appreciate the useful discussion of the results with Dr. Dezhang Chu from Woods Hole Oceanographic Institution and two anonymous reviewers. The work was partially sponsored by the Institute of Oceanology, Polish Academy of Sciences (the sponsor programme 2.7) and by the Research Council of Norway (Grant No. 143249/140).

References

Blaxter, J. H. S. 1979. The herring swimbladder as a gas reservoir for the acoustico-lateralis system. Journal of the Marine Biological Association of the United Kingdom, 59: 1–10.

Blaxter, J. H. S., and Batty, R. S. 1984. The herring swimbladder: loss and gain of gas. Journal of the Marine Biological Association of the United Kingdom, 64: 441–459.

Dragesund, O., Hamre, J., and Ulltang, Ø. 1980. Biology and population dynamics of the Norwegian spring-spawning herring. Rapports et Procès-Verbaux des Réunions Conseil International pour l'Exploration de la Mer, 177: 43–71.

Gorska, N., and Ona, E. 2003. Modelling the acoustic effect of swimbladder compression in herring. ICES Journal of Marine Science, 60: 548–554.

Huse, I., and Ona, E. 1996. Tilt-angle distribution and swimming speed of overwintering Norwegian spring-spawning herring. ICES Journal of Marine Science, 53: 863–873.

Johannessen, A., Slotte, A., Bergstad, O. A., Dragesund, O., and Røttingen, I. 1995. Re-appearance of Norwegian spring-spawning herring (*Clupea harengus* L.) at spawning grounds off southwestern Norway. *In* Ecology of Fjords and Coastal Waters, pp. 347–363. Ed. by H. R. Skjoldal, C. Hopkins, K. E. Erikstad, and H. P. Leinoas. Elsevier Science B.V., Amsterdam.

Ona, E. 1990. Physiological factors causing natural variations in acoustic target strength of fish. Journal of the Marine Biological Association of the United Kingdom, 70: 107–127.

Ona, E. 2003. An expanded target-strength relation for herring. ICES Journal of Marine Science, 60: 493–499.

Ona, E., Svellingen, I., and Fosseidengen, J. E. 2001. Target strength of herring during vertical excursions, pp. 1–16. ICES Fisheries Acoustics, Science and Technology Working Group (FAST), Seattle, April 2001.

Ona, E., Vabø, R., Huse, I., and Svellingen, I. Depth-dependent target strength in herring. ICES Journal of Marine Science, submitted for publication.

Røttingen, I., Foote, K. G., Huse, I., and Ona, E. 1994. Acoustic-abundance estimation of wintering Norwegian spring-spawning herring with emphasis on methodological aspects. ICES CM 1994/(B + D + G + H): 1 (Mimeo).

Stanton, T. K. 1989. Sound scattering by cylinder of finite length. III. Deformed cylinders. Journal of the Acoustical Society of America, 86: 691–705.

Vabø, R. 1999. Measurements and correction models of behaviourally induced biases in acoustic estimates of wintering herring (*Clupea harengus* L.). Thesis, Dr. Scient. University of Bergen.